Biostructural Models for the Binding of Nucleoside Analogs to SARS-CoV-2 RNA-Dependent RNA Polymerase

Andrew J. Prussia* and Spandan Chennamadhavuni

Cite This: https://dx.doi.org/10.1021/acs.jcim.0c01277
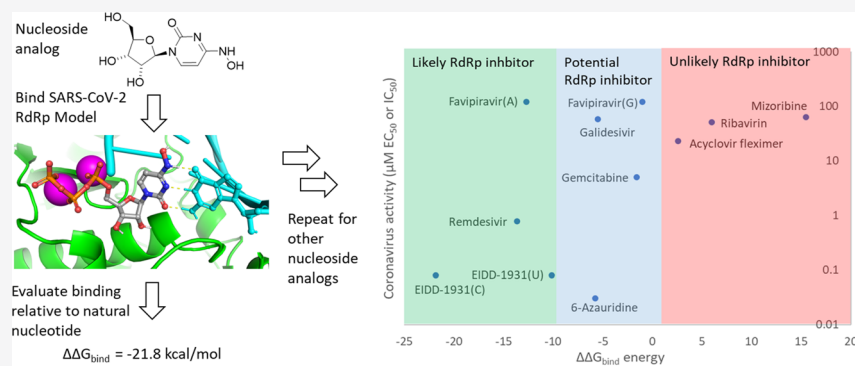
Read Online

ACCESS | Metrics & More | Article Recommendations | Supporting Information

ΔΔG_bind = -21.8 kcal/mol

ABSTRACT: SARS-CoV-2 is a positive-sense RNA virus that requires an RNA-dependent RNA polymerase (RdRp) for replication of its viral genome. Nucleoside analogs such as Remdesivir and β-D-N^4-hydroxycytidine are antiviral candidates and may function as chain terminators or induce viral mutations, thus impairing RdRp function. Recently disclosed Cryo-EM structures of *apo*, RNA-bound, and inhibitor-bound SARS-CoV-2 RdRp provided insight into the inhibitor-bound structure by capturing the enzyme with its reaction product: Remdesivir covalently bound to the RNA primer strand. To gain a structural understanding of the binding of this and several other nucleoside analogs in the precatalytic state, molecular models were developed that predict the noncovalent interactions to a complex of SARS-CoV-2 RdRp, RNA, and catalytic metal cations. MM-GBSA evaluation of these interactions is consistent with resistance-conferring mutations and existing structure−activity relationship (SAR) data. Therefore, this approach may yield insights into antiviral mechanisms and guide the development of experimental drugs for COVID-19 treatment.

INTRODUCTION

The pandemic of COVID-19 has brought much of the world to a halt.[1] Its causative agent, SARS-CoV-2, is a betacoronavirus thought to have made an interspecies jump from endemic infection in bats to respiratory infection in humans.[2] From an evolutionary selection viewpoint, the virus is tremendously successful, striking a balance between contagiousness and lethality that has allowed it to escape central China and spread throughout the world. As of today, over 100 million people have been infected and over 2.2 million people have died worldwide.[3] Its human toll has been enormous, and a massive global effort is underway to identify and evaluate vaccines, antiviral agents, and immunotherapies.[4] Although some of the treatment options are now available under emergency use approvals for limited populations, public health efforts are still limited to centuries-old methods of limiting exposure: social distancing, handwashing, protective equipment, and quarantine.[5]

This is not the first coronavirus to threaten mankind. The closest relative to SARS-CoV-2 that causes disease in humans is SARS-CoV, now known as SARS-CoV-1.[2] Its outbreak in 2003−2004 was limited to Asia, but the fatality rate was much higher, around 10%.[6] There have been several attempts to develop an antiviral drug for SARS-CoV-1, and while some showed promise, without an ongoing outbreak, no treatment was finalized.[6] Unlike the positive-sense RNA virus SARS-CoV-2, Ebolavirus is a negative-sense RNA virus but went through a similar antiviral development cycle: without the pressure from an uncontrollable spread, no antiviral drugs were approved.[7] Fortunately, these efforts did leave us with late-stage experimental drugs that could be repurposed against SARS-CoV-2.[8] One class of these repurposed antiviral drugs that have shown activity against SARS-CoV-2 are nucleoside analogs (Figure 1).[9−11] Coronaviruses, Filoviruses (such as Ebola virus) and other single-stranded RNA viruses require an RNA-dependent RNA polymerase (RdRp) for replication of
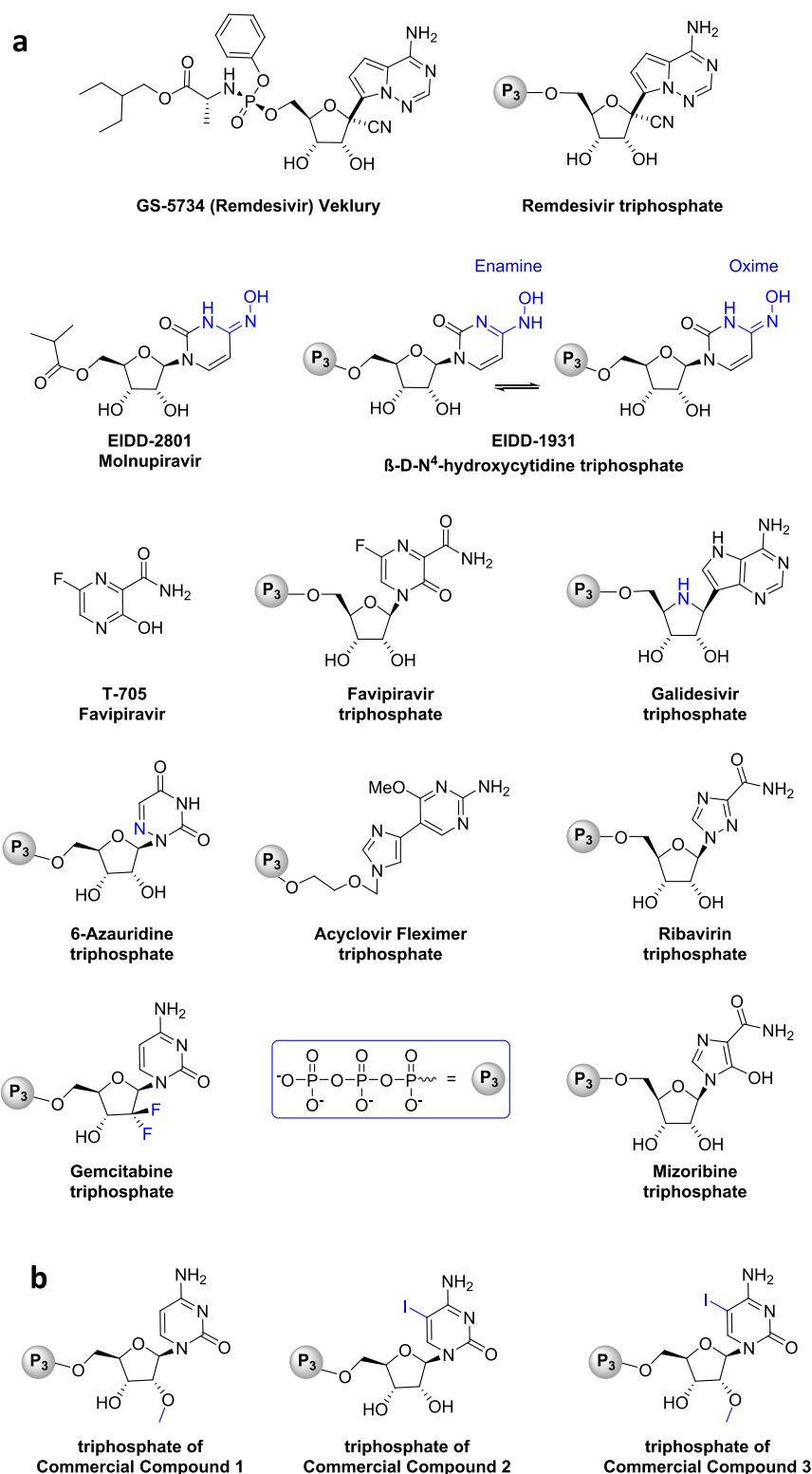
Figure 1. (a) Nucleoside analogs with known antiviral activity against SARS-CoV-2 are shown in their dosed and metabolically active forms. (b) Commercially available compounds **1**, **2**, and **3** are predicted to be RdRp inhibitors in their triphosphorylated form.

their genomes. The catalytic cores of these enzymes are remarkably conserved across the virus families since the basic functions of holding viral RNA, binding an incoming ribonucleotide, and catalyzing the polymerase reaction are necessary steps in all these viral families.[12] It may even be possible for a nucleoside analog to have activity against multiple viral families and thus function as frontline therapy in the next outbreak.[13,14]

Although the RdRp of SARS-CoV-2 is an attractive target, effective inhibition by nucleoside analogs requires a complicated sequence of metabolic transformations because the active agent is not the nucleoside analog. It is instead the nucleoside triphosphate (NTP) that is needed for its
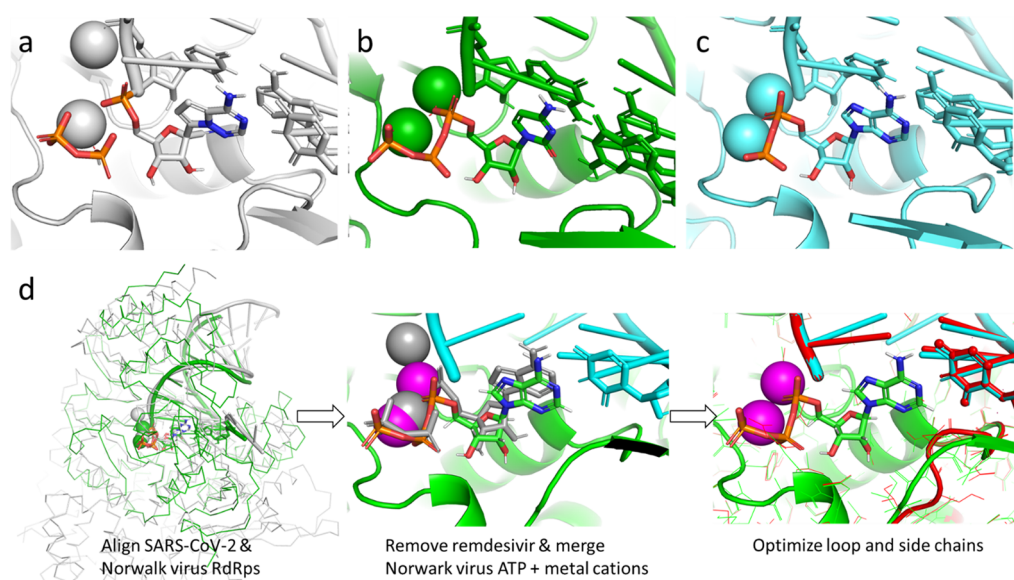
B

Figure 2. Experimental structures for (a) SARS-CoV-2, (b) Norwalk virus, and (c) HCV polymerases. Remdesivir/pyrophosphate, nucleotides, and adjacent RNA are displayed as sticks (heteroatoms are colored in Remdesivir or the incoming nucleotide). Metals are shown as spheres. (d) Development of the SARS-CoV-2 RdRp model complex in three steps: (1) SARS-CoV-2 (gray) and Norwalk virus (green) RdRps were aligned. (2) Remdesivir/metals (gray) were removed and replaced with ATP/metals (green carbons, magenta metals) from Norwalk virus RdRp. (3) Loop 676-686 and side-chain rotamers were optimized to the new nucleotide/metal positions. The unoptimized structure is shown in red.

incorporation into the viral RNA. Such a charged species, however, would have limited absorption and distribution across cellular membranes.[7,9−11] As a consequence, nucleoside drugs are either dosed as nucleoside analogs (*i.e.*, the compound possesses a free 5′-hydroxyl) or as monophosphate prodrugs, both of which typically possess good cellular permeability. In the former case, three different cellular kinases sequentially phosphorylate the 5′-hydroxyl to produce the desired NTP. In the latter case, endogenous enzymes (esterases, phospholipases, phosphoramidases, etc.) unravel the prodrug to reveal the nucleoside monophosphate. The first phosphorylation step, which is often rate-limiting, is then followed by kinetically favored second and third phosphorylation steps. In order for the NTP to inhibit viral replication, it must inhibit the RdRp from functioning. If the NTP−RdRp interaction is favorable, it will be incorporated into a growing strand of RNA and either terminate its elongation or cause it to become dysfunctional. All these steps are necessary but not sufficient for the nucleoside analog in question to be a viable antiviral agent. The final hurdle relates to the safety of the nucleoside analog, *i.e.*, it must exhibit a binding preference at the viral RdRp over cellular nucleotidyl receptors.

As there was no structural information available, we initially built a homology model for SARS-CoV-2 RdRp based on structural information for other positive-sense, single-strand RNA viruses. Recently, however, cryo-electron microscopy structures have been reported for coronaviruses: an *apo* RdRp structure (PDB code 6M71),[15] an RdRp with duplex RNA bound (PDB code 6YYT),[16] and an RdRp structure covalently bound to Remdesivir (PDB code 7BV2),[17] which dramatically advanced our knowledge of the SARS-CoV-2 RdRp complexes. The three studies found structures that closely matched the SARS-CoV-1 RdRp structure (PDB code 6NUR) published last year, which is not surprising given their 96% sequence identity.[18] However, *apo* RdRp structures are of limited utility for the binding rationalization of nucleoside analogs that require base-pairing to the template RNA strand to function as

inhibitors. Likewise, the RNA-bound and Remdesivir-bound structures are also not ideal because both are reaction products of enzymatic catalysis and not the precatalytic state where nucleoside analogs must compete with endogenous nucleotides as substrates for the polymerization reaction. Multiple structural features differ between the Remdesivir structure and initialization complexes for other viral RdRps including the positions of catalytic metals, aspartate side chains, and the conformation of a loop interacting with template RNA (Figure 2a−c).[19−21]

Ahmad and colleagues used homology modeling and other computational techniques with the structures described above to investigate possible small-molecule inhibition of the SARS-CoV-2 RdRp initiation complex with GTP.[22] Although this approach may provide inhibitors for the initiation stage without primer-bound RNA, the primary inhibitory mechanism by Remdesivir and other nucleoside analogs is delayed chain termination at the *i* + 3 position.[23,24] Gordon et al.[23] demonstrated this mechanism through enzyme kinetics and developed a structural model for noncovalent interaction of Remdesivir but did not rationalize existing SAR data. Independently, we built precatalytic biostructural models for SARS-Cov-2 RdRp to evaluate the binding of Remdesivir and many other antiviral drugs of SARS-CoV-2 RdRp such as *β*-D-N[4]-hydroxycytidine,[13,25] Favipiravir,[26] and other potential nucleoside analog inhibitors.[27] These models were developed with the complementary template RNA nucleobases to accommodate nucleoside analogs with different nucleobases. A mutated version of SARS-CoV-2 RdRp with resistance to Remdesivir was also developed. Using these models, the potential binding of phosphorylated nucleoside analogs was evaluated using the MM-GBSA protocol and compared with the binding of natural RNA nucleotides. The obtained results show that the models are beneficial in developing the next generation of nucleoside analogs against SARS-CoV-2.

■ METHODS

Development of SARS-CoV-2 RdRp-RNA-Metal Complexes. The 2.5 Å resolution electron microscopy structure of the SARS-CoV-2 nsp12-nsp7-nsp8 (PDB code 7BV2, Figure 2a)[18] was aligned with the 1.8 Å X-ray crystallography structure of the Norwalk virus polymerase (PDB code 3BSO, Figure 2b)[19] using the Protein Structure Alignment tool by Schrödinger, LLC.[28] This tool aligns the secondary structure features that are common to the two proteins. The overall RMSD in C-alpha positions was 3.2 Å with an alignment score of 0.47 (alignment scores <0.6 indicate good alignment; proteins with >0.8 scores may not be similar structurally).[29] Although the sequence homology between these two proteins is low with this alignment (8% identity, 19% similarity), the binding site residues are conserved with residues within 5 Å having an 1.6 Å RMSD in their C-alpha atom positions and the conserved viral RdRp motifs A, B, C, and D overlapping (the E and F motifs are not available in the 3BSO structure).[30] To create the precatalytic model, Remdesivir and the catalytic metal cations of 7BV2 were replaced with ATP and the catalytic metal cations of the aligned structure of 3BSO. The resulting structure was prepared for molecular calculations and evaluated for steric clashes and other issues by the Protein Preparation Wizard.[31] With the geometry of ATP, RNA, and metal cations fixed in a precatalytic state, loop refinement of residues forming the 676-686 loop and side-chain predictions of all residues were performed with Prime using the VSGB continuum solvation model for water and the OPLS3 force field.[32,33] Extended serial loop sampling was chosen during loop refinement to ensure that sufficient sampling was performed to identify the lowest-energy loop conformation. We hypothesized that optimizing the enzyme around a precatalytic state of its substrate would shift its conformation to a state suitable for nucleoside analog binding.

Optimization of Nucleoside Analogs with the MM-GBSA Protocol. With the structure optimized toward a precatalytic state with ATP bound, other nucleoside analogs were modeled by modifying the ATP ribose and base rings to the desired substituents. To model GTP, CTP, UTP, and the nucleoside analogs that mimic these bases, the template RNA base was mutated to the complementary base. The modified structures were created in chemically reasonable conformations to avoid high-energy contacts upon optimization. Optimization calculations were performed with the Prime MM-GBSA protocol using the same solvation and force field settings as above.[32,33] The ligand (ATP, GTP, CTP, UTP, or the nucleotide analogs) was allowed complete flexibility, while the protein, RNA, and metal cations within 6 Å of the ligand were flexible with harmonic constraints of 1.0 kcal/mol·Å^2. The difference in MM-GBSA ΔG (NS) binding energies ($\Delta\Delta G_{bind}$) was calculated by subtracting the binding energy of the natural nucleotide (that expected to be displaced in the active site) from the binding energy of the nucleoside analog of interest.

Density Functional Theory Calculations for Tautomers of EIDD-1931. The energy difference between the enamine and oxime forms of EIDD-1931 was calculated on *N*-methyl model systems of the nucleobase by optimization using Jaguar at the M06-2X/cc-pVTZ(-f) level with the Poisson–Boltzmann continuum water solvation model.[34] The *N*-methyl model system of the nucleobase was used to (1) reduce calculation time, (2) r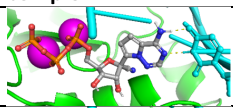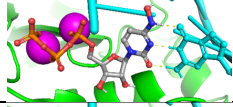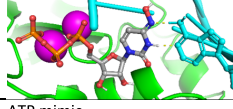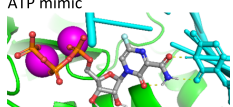emove alternative conformations, which would confound the final energy but not the tautomerization equilibrium, and (3) focus on subtle differences in the energies of tautomers in the solution phase. The stereoelectronic effect of the sugar or the triphosphate group is expected to be negligible in the tautomerization equilibrium of the binding conformation of EIDD-1931.
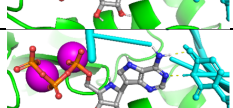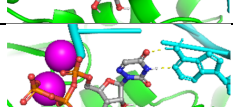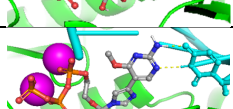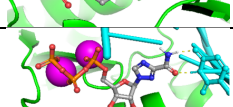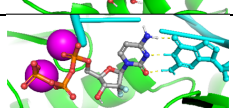
■ RESULTS AND DISCUSSION

The starting point for building this model was the 2.8 Å resolution electron microscopy structure of the SARS-CoV-2 nsp12-nsp7-nsp8 with Remdesivir covalently bound (Figure 2a).[17] This structure was modified into a precatalytic state by removing Remdesivir from the primer RNA and inserting adenosine triphosphate (ATP) into the state captured by the 1.7 Å resolution X-ray crystallography structure of the Norwalk virus RdRp initiation complex (PDB code 3BSO, Figure 2b).[19] The Norwalk virus RdRp structure was chosen because of its structural similarity to SARS-CoV-2 and its unique capture of the triphosphate form of a nucleo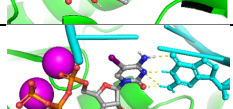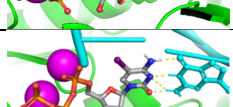tide instead of the diphosphate form of HCV (Figure 2c). The two catalytic metals were also shifted to the position found in the Norwalk virus RdRp. Once in place, a slight shift in the 676-686 loop was necessary to accommodate the nucleotide in this state. This was remedied by a loop prediction algorithm and resulted in a subtle conformational change of this loop. The protein side chains were also optimized to this form by a side-chain prediction algorithm, which converged on a low-energy conformation that mimics the precatalytic state found in the Norwalk and Hepatitis C Virus RdRp structures (Figure 2b,c).[19−21] Similar side-chain rotamers and loop conformations indicate that these refinement procedures have shifted the enzyme from a post- to a precatalytic form observed for the Norwalk virus RdRp. An overview of the modeling process is illustrated in Figure 2d. Our biostructural model would be extremely beneficial in prioritizing novel nucleoside analogs, while structural biologists experiment with methodologies to capture the SAR-CoV-2 RdRp in its precatalytic state using X-ray crystallographic or cryo-electron microscopy methods.

The energetics of the resulting complex can be interrogated by the MM-GBSA binding energy procedure.[32,33] Although other computational methods such as free energy of perturbation (FEP) or hybrid QM/MM could be applied, our focus was on (a) maintaining the proper geometry for the polymerase reaction and (b) a method that could be applied rapidly to many nucleoside analogs. This is a reasonable approach to predict inhibition of nucleoside analogs, considering other inherent variables such as phosphorylation and ADMET. This protocol allowed the nucleotide to freely optimize its structure in the presence of the protein, duplex RNA, and metal cations. If there were unfavorable interactions between this substrate and the surrounding atoms, it was anticipated that the structure might become distorted or the nucleotide would be pushed out of the catalytic binding pocket. However, with this approach, the nucleotide maintained its conformation, shifting slightly in position but maintaining base-pair interactions with the template strand of RNA, indicating that its binding pose may be similar to the initial stage of the polymerase reaction (Figure 2c). The metal cations also shifted slightly in their position while maintaining coordination interactions with the catalytic aspartate side chains. The MM-GBSA protocol provided a calculated binding interaction energy. Because this energy is dominated by the electrostatic term from the charged interactions between the

Table 1. Nucleoside Anti-Coronavirus Activity and Predicted Binding in the Active Site of the SARS-CoV-2 RdRp Model Complex

Nucleoside analog	Binding pose in SARS-CoV-2 RdRp model complex	Antiviral activity[b]	$\Delta\Delta G_{bind}$[a] (kcal/mol)
Remdesivir triphosphate		0.77 µM: SARS-CoV-2 EC$_{50}$ 0.069 µM: SARS-CoV-1 IC$_{50}$ 0.074 µM: MERS-CoV IC$_{50}$	-13.6
EIDD-1931 triphosphate (enamine tautomer)		0.08 µM: SARS-CoV-2 IC$_{50}$ 0.14 µM: SARS-CoV-1 IC$_{50}$ 0.024 µM: MERS-CoV IC$_{50}$	-21.8
EIDD-1931 triphosphate, (oxime tautomer)			-10.11
Favipiravir triphosphate	ATP mimic	118.3 µM: SARS-CoV-2 IC$_{50}$ (CPE) 207.1 µM: SARS-CoV-2 IC$_{50}$ (replication)	-12.7
	GTP mimic		-1.0
Galidesivir triphosphate		57.7 µM: SARS-CoV-1 EC$_{50}$ 68.4 µM: MERS-CoV-1 EC$_{50}$	-5.5
6-Azauridine triphosphate		0.03 µM: HCoV-NL63 IC$_{50}$	-5.73
Acyclovir fleximer triphosphate		23 µM: MERS-CoV IC$_{50}$ 8.8 µM: HCoV-NL63 IC$_{50}$	+2.6
Ribavirin triphosphate		50-819 µM: SARS-CoV-1 IC$_{50}$ 20 µM: MERS-CoV IC$_{50}$	+6.0
Gemcitabine triphosphate		1.22 µM: MERS-CoV IC$_{50}$ 4.96 µM: SARS-CoV-1 IC$_{50}$	-1.56
Mizoribine triphosphate		13.5 µM: MERS-CoV IC$_{50}$ 62 µM: SARS-CoV-1 IC$_{50}$	+15.5
Commercial compound 1		Not yet available	-13.5
Commercial compound 2		Not yet available	-16.8
Commercial compound 3		Not yet available	-16.3

[a]Energies described by $\Delta\Delta G_{bind}$ are relative to the natural nucleotide predicted to be displaced by the nucleoside analog. [b]Antiviral efficacies against SARS-CoV-2, SARS-CoV-1, MERS-CoV, and HCoV-NL63.[9,13,25,36,37,39−42]

nucleotide phosphates, catalytic metals, and negatively charged aspartate side chains (the Coulombic term is >3 times the vdW term but countered by the solvation term), it is not expected to give an accurate absolute binding energy that would be

correlated with antiviral activity. It could, however, provide relative energies to compare the binding of nucleotide analogs with the same nucleobase or bioisostere. This is described as $\Delta\Delta G_{bind}$, which compared the binding energy of a nucleotide analog with its respective natural nucleotide (Table 1). Because this competitive binding is one of the many conditions necessary to achieve viral inhibition, this energetic comparison is unlikely to be correlated with antiviral activity but could provide a basis for SAR comparison between analogs that could classify analogs into three categories: (a) likely RdRp inhibitors, (b) potential RdRp inhibitors, and (c) unlikely RdRp inhibitors. This virtual evaluation approach might be advantageous in prioritizing which nucleosides to screen for their antiviral efficacy, given the limited synthesis and virology resources.

Remdesivir (Veklury) is the first FDA-approved drug for Covid-19 treatment.[35] It was discovered and developed by Gilead Pharmaceuticals and has completed eight phase 3 clinical trials. Currently in 49 active or recruiting phase 3 clinical trials, it is a phosphoramidate prodrug C-nucleoside analog with both a modified nucleobase and ribose sugar (Figure 1).[27,36,37] Its base mimics the hydrogen bond pairing of adenosine, but its ribose has a 1′-nitrile substituent distinct from the natural nucleotide. To dock its respective nucleotide into the SARS-CoV-2 RdRp complex, ATP was modified in place to Remdesivir and the complex was subjected to MM-GBSA minimization. The resulting structure showed a slight shift in position but established a polar contact between the 1′-nitrile substituent and Ser759 while maintaining strong base-pairing hydrogen bonds with the template RNA nucleobase (Table 1). Notably, the 1′-nitrile interaction was different in the covalently bound Remdesivir structure, which had a polar interaction to Thr687. Compared with ATP, Remdesivir had a more favorable MM-GBSA binding energy by −13.1 kcal/mol. This is consistent with Remdesivir's high level of antiviral activity and kinetic assays, which show that the enzyme is more selective for Remdesivir over ATP.[23]

The ribonucleoside analog β-D-N^4-hydroxycytidine (NHC, EIDD-1931) is only modified from cytidine by an oxime at the 4 position of the nucleobase (Figure 1),[25] yet it showed antiviral efficacy against a panel of viruses, including SARS-CoV-2. Its 5′-isopropyl ester prodrug, Molnupiravir (EIDD-2801) was found to have better ADMET and is orally bioavailable.[13] Currently, the drug is in two phase 3 clinical trials (NCT04575584 and NCT04575597). The oxime also tautomerizes to the enamine form. Interestingly, this provides the analog with two base-pairing opportunities: the oxime tautomer mimics uridine, while the enamine imitates cytidine.[38] Optimization of both tautomer nucleobases at the M06-2X/cc-pVTZ(-f) level with the Poisson−Boltzmann continuum water solvation method indicated near equivalent populations of both tautomers. It was found that the oxime form is slightly favored by 0.2 kcal/mol in the solution phase (although the tautomerization equilibrium could be shifted upon binding with the enzyme). Analyses of the active triphosphorylated forms of both tautomers in the SARS-CoV-2 RdRp model complex revealed nearly identical positioning to natural uridine and cytidine, but with an additional hydrogen-bonding interaction between the enamine or oxime hydroxyls with the preceding base in the primer RNA strand (Table 1). The MM-GBSA protocol calculated binding energies −21.8 and −10.1 kcal/mol relative to the binding of unmodified uridine and cytidine, respectively, consistent with the potent

broad-spectrum antiviral efficacy of this nucleoside analog. This also indicates that nucleoside analogs to bases other than ATP can be evaluated in this model system. It is important to note that although both the DFT and the MM-GBSA calculations give energy results in kcal/mol, the MM-GBSA calculations are based on molecular mechanics and are not expected to give thermodynamically accurate energies in this system.

Favipiravir (Figure 1) is unique from all other nucleoside analogs discussed earlier as it is dosed in substituted pyrimidine form. Once in the cell, Favipiravir undergoes phosphoribosylation to the active antiviral form Favipiravir ribofuranosyl-5′-triphosphate.[39] The modified pyrimidine ring of Favipiravir is a unique bioisostere of adenosine or guanosine in its base-pairing hydrogen bonding capability. In the SARS-CoV-2 RdRp model complex, Favipiravir RTP retained a similar position to either natural adenosine or guanosine nucleotides but formed more favorable interactions when acting as an adenosine mimic (Table 1). The binding energy relative to adenosine is −12.7 kcal/mol, suggesting that binding to the SARS-CoV-2 RdRp could be favorable. Favipiravir does in fact inhibit SARS-CoV-2 through this mechanism with an IC_{50} of 118.3 μM, as was recently reported.[26] This level of inhibition may be due to phosphoribosylation steps, which could limit the supply of the active ribofuranosyl-5′-trisphosphate form.

Galidesivir (BCX4430) (Figure 1) is currently being evaluated in the clinical trials for COVID-19 (NCT03891420) by BioCryst Pharmaceuticals. This experimental drug is an adenosine nucleoside analog, containing a slightly modified base and an aza sugar. It has broad-spectrum activity against nine virus families with 57.7 and 68.4 μM EC_{50} against SARS-CoV-1 and MERS-CoV, respectively.[40] When docked in the SARS-CoV-2 RdRp complex, it is predicted to have moderately favorable interaction based on a $\Delta\Delta G_{bind}$ energy of −5.5 kcal/mol. Thus, relative binding energies in the range of −5 to −10 kcal/mol may represent analogs with the modest activity.

6-Azauridine (Figure 1) has 0.03 μM EC_{50} activity against a human coronavirus NL63 (HCoV-NL63), another pathogenic virus associated with acute respiratory illness.[41] The overall sequence similarity between the RdRps of HCoV-NL63 and SARS-CoV-2 is moderate (37% identity, 53% homology), so a common inhibition is possible. Evaluation in the model of SARS-CoV-2 RdRp predicts an interaction similar to Galidesivir, with a $\Delta\Delta G_{bind}$ energy of −5.7 kcal/mol.

The model did not predict favorable binding for an Acyclovir Fleximer, while this nucleoside analog has 23 and 8.8 μM EC_{50} activities against MERS-CoV and HCoV-NL63, respectively.[41] This biaryl compound was designed to not only mimic a purine hydrogen bonding pattern but also be able to adopt alternative binding modes.[42] In the model, the compound was only able to fit in the catalytic site as an adenosine mimic, base pairing with the uracil base of the template RNA, but it is possible that the compound may function as another nucleobase mimic or adopt an alternative binding mode. This compound has not yet been shown experimentally to function as a chain terminator (either immediate or delayed) of RNA replication, so it may function by a mechanism that does not require RNA incorporation. Since our models are based on competition with natural nucleotides in a precatalytic state, it might not be able to predict other inhibition mechanisms. An additional kinetic

assay or structural information for this compound may be necessary to elucidate its inhibition mechanism.

Ribavirin is another nucleoside analog with broad-spectrum activity but is thought to act pleiotropically by inhibiting the host inosine monophosphate dehydrogenase, increasing expression of interferon-gamma and tumor necrosis factor-alpha and increasing the frequency of viral mutations.[9] Only the latter mechanism would require direct binding of Ribavirin triphosphate with the SARS-CoV-2 RdRp complex, but the effect could be negated by the exoribonuclease proofreading function of beta coronaviruses.[6] In SARS-CoV-1, Ribavirin triphosphate is known to be incorporated, but then excised by this function, making this mechanism unlikely to play a role in ribavirin inhibition of the SARS-CoV-2 virus. In an enzyme kinetics study, the K_m for Ribavirin triphosphate binding is 136 μM for SARS-CoV-1 RdRp, 4-fold higher than Remdesivir triphosphate.[23,43] The $\Delta\Delta G_{bind}$ energy for Ribavirin triphosphate is +6.0 kcal/mol, indicating that the model may not identify weak binding interactions even if the nucleotide analog is capable of RNA incorporation.

Mizoribine and Gemcitabine also are active against coronaviruses, SARS-CoV and MERS-CoV, at micromolar levels.[41] Gemcitabine is only predicted to have a slightly favorable interaction in the SARS-CoV-2 model, with a $\Delta\Delta G_{bind}$ energy of −1.56 kcal/mol, while Mizoribine is disfavored by 15.5 kcal/mol. The mechanism of viral inhibition is not confirmed for either of these nucleoside analogs: Gemcitabine is a chemotherapy drug and Mizoribine is an immunosuppressant, so it is possible that their antiviral activities are due to host-directed inhibition rather than direct interaction with a viral protein. Figure 3 summarizes the
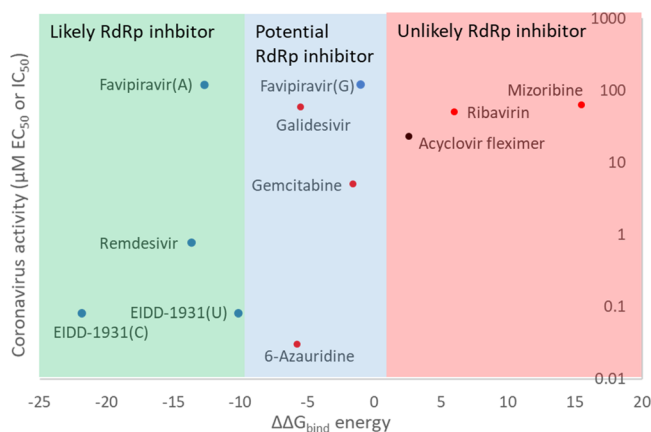

Figure 3. Graph of coronavirus inhibition of nucleoside analogs versus their $\Delta\Delta G_{bind}$ energies evaluated in the SARS-CoV-2 RdRp model. Blue, red, and black circles indicate SARS-CoV-2, SARS-CoV-1, and MERS-CoV-1 inhibition activities, respectively. Coronavirus activities on the y-axis are log-scaled.

relationship between coronavirus inhibition from SARS-CoV-2, SARS-CoV-1, or MERS-CoV-1 and binding energies in the model (the coronavirus most similar to SARS-CoV-2 with available inhibition data is shown). Nucleoside analogs with documented RdRp inhibition are predicted to have favorable binding relative to the natural nucleotide. Analogs with $\Delta\Delta G_{bind}$ energies more favorable than −10 kcal/mol are often active at sub-micromolar levels against coronaviruses. The model may therefore be useful to prioritize synthetic and biological resources for developing nucleoside analogs against

coronaviruses, along with the necessary considerations of ADMET properties, phosphorylation, and synthetic feasibility. The complex cellular and viral interactions necessary for nucleoside analog inhibitions preclude a quantitative prediction of antiviral activity using this model, but the model may serve to classify nucleoside analogs as probable, possible, or unlikely SARS-CoV-2 RdRp inhibitors. To demonstrate the utility of this approach, commercially available nucleoside analogs from the Granlen library (Granlen, Inc.) were evaluated in the models. Examples of likely RdRp inhibitors are shown in Table 1. The model predicts that 2′-methoxy substitution (Commercial Compound **1**) and iodo-substitution at the 5-position of the cytosine nucleobase (Commercial Compound **2**) are favorable ($\Delta\Delta G_{bind}$ energies of −13.5 and −16.8 kcal/mol, respectively). Although both substitutions appear to be compatible in one compound (Commercial Compound **3**), there seems to be no apparent additive effect on the binding energy ($\Delta\Delta G_{bind}$ energy of −16.3 kcal/mol). These and other commercially available nucleoside analogs, as well novel entities, continue to be investigated by our research group.

Mutations conferring resistance are a hallmark of RNA viruses under antiviral pressure, even with coronaviruses that also have an exonuclease proofreading functionality. The two mutations that have been observed against Remdesivir in SARS-CoV-1 are Phe480Leu and Val557Leu and result in a 5.6-fold decrease in inhibition.[14,44] These mutations were modeled in the SARS-CoV-2 RdRp model and the complex subjected to the side-chain prediction of all protein residues. The complex converged on an almost identical arrangement of side chains (Figure 4). Subjecting Remdesivir to the MM-GBSA protocol in the mutated model did not cause a significant difference in the binding pose but did reduce $\Delta\Delta G_{bind}$ to −0.3 kcal/mol. It appears that extending the isopropyl group of Val557 to isoleucine forces this nonpolar residue near the more polar aromatic ring of Remdesivir. The Phe480Leu mutation is distal to the active site and RNA binding residues. This mutation may play a role in the dynamics of the polymerase as it opens and closes in the process of binding RNA and catalyzing the polymerase reaction. Resistance-conferring mutations to Remdesivir have not yet been observed in SARS-CoV-2 RdRp but are likely to occur through the same mechanisms based on the 96% sequence identity between the RdRps of these viruses. Interestingly, EIDD-1931 maintains its activity against a coronavirus RdRp bearing these mutations.[13] Its $\Delta\Delta G_{bind}$ in the enamine tautomer reduced to −5.6 kcal/mol but was still in the range of possibly active nucleoside inhibitors similar to Galidesivir.

■ CONCLUSIONS

The development of biostructural models for SARS-CoV-2 RdRp has enabled the virtual evaluation of nucleoside analogs for antiviral activity. Known nucleoside analog inhibitors, such as Remdesivir and Molnupiravir, are predicted to bind favorably in the precatalytic models of the RdRp, demonstrating that multiple nucleobase and ribose substitutions can be evaluated by the models with correct activity classification. Models with mutations that confer resistance to Remdesivir are able to quantify a structural rationale for this effect that is consistent with the absence of resistance to Molnupiravir. With these tools, commercially available nucleoside analogs with potential anti-coronavirus activity were identified and
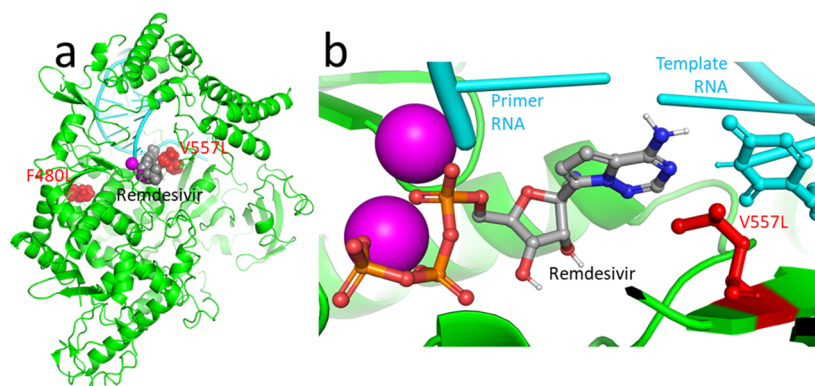
Figure 4. Resistance-conferring mutations in the SARS-CoV-2 RdRp model complex. (a) Position of the mutations relative to the Remdesivir-bound active site. The F480L mutation is distal to the active site and RNA-binding domains, but the V557L mutation interacts directly with the active site. (b) The V557L mutation increases contact between the nonpolar residue and the modified base of Remdesivir.

prioritized for testing. The authors will continue these efforts to aid other researchers in the development of nucleoside analogs against the global pandemic of COVID-19. All modeled structures described here are available for download in Supporting Information 1−4. While safe and effective (>95%) vaccines (Pfizer, Moderna, etc.) against SARS-CoV-2 are now available, inoculating the world population is a costly, time-taking endeavor. Limited vaccine availability, logistics in distribution, compliance issues, and emerging variants of viruses due to mutations mean that novel direct-acting antivirals will still be necessary to tackle this ongoing pandemic as well as threats that mankind might face in the future. The authors aspire that these models, along with efforts to develop different classes of antivirals, vaccines, and other therapies, will facilitate a global solution to the current crisis.

ASSOCIATED CONTENT

ⓈⒾ Supporting Information

The Supporting Information is available free of charge at https://pubs.acs.org/doi/10.1021/acs.jcim.0c01277.

PDB files for the optimized nucleoside analog complexes for atp (ZIP)

PDB files for the optimized nucleoside analog complexes for ctp (ZIP)

PDB files for the optimized nucleoside analog complexes for utp (ZIP)

PDB files for the optimized nucleoside analog complexes for gtp (ZIP)

AUTHOR INFORMATION

Corresponding Author

Andrew J. Prussia − *Department of Chemistry, Emory University, Atlanta, Georgia 30322, United States;* ⓞ orcid.org/0000-0002-7038-9520; Email: aprussia@me.com.

Author

Spandan Chennamadhavuni − *Department of Chemistry, Emory University, Atlanta, Georgia 30322, United States;* ⓞ orcid.org/0000-0002-1026-9527

Complete contact information is available at:
https://pubs.acs.org/10.1021/acs.jcim.0c01277

Notes

The authors declare no competing financial interest.

REFERENCES

(1) Fauci, A. S.; Lane, H. C.; Redfield, R. R. Covid-19 - Navigating the Uncharted. *N. Engl. J. Med.* **2020**, *382*, 1268−1269.

(2) Andersen, K. G.; Rambaut, A.; Lipkin, W. I.; Holmes, E. C.; Garry, R. F. The Proximal Origin of SARS-CoV-2. *Nat. Med.* **2020**, *26*, 450−452.

(3) Dong, E.; Du, H.; Gardner, L. An Interactive Web-Based Dashboard to Track COVID-19 in Real Time. *Lancet Infect. Dis.* **2020**, *20*, 533−534.

(4) Kupferschmidt, K.; Cohen, J. Race to find COVID-19 treatments accelerates. *Science* **2020**, *367*, 1412−1413.

(5) CDC. *Implementation of Mitigation Strategies for Communities with Local COVID-19 Transmission*; Atlanta, 2020.

(6) de Wit, E.; van Doremalen, N.; Falzarano, D.; Munster, V. J. SARS and MERS: Recent Insights into Emerging Coronaviruses. *Nat. Rev. Microbiol.* **2016**, *14*, 523−534.

(7) De Clercq, E. New Nucleoside Analogues for the Treatment of Hemorrhagic Fever Virus Infections. *Chem. - An Asian J.* **2019**, *14*, 3962−3968.

(8) Morse, J. S.; Lalonde, T.; Xu, S.; Liu, W. R. Learning from the Past: Possible Urgent Prevention and Treatment Options for Severe Acute Respiratory Infections Caused by 2019-NCoV. *ChemBioChem* **2020**, *21*, 730−738.

(9) Jordan, P. C.; Stevens, S. K.; Deval, J. Nucleosides for the Treatment of Respiratory RNA Virus Infections. *Antiviral Chem. Chemother.* **2018**, *26*, 1−19.

(10) Yates, M. K.; Seley-Radtke, K. L. The Evolution of Antiviral Nucleoside Analogues: A Review for Chemists and Non-Chemists. Part II: Complex Modifications to the Nucleoside Scaffold. *Antiviral Res.* **2018**, *162*, 5−21.

(11) Seley-Radtke, K. L.; Yates, M. K. The Evolution of Nucleoside Analogue Antivirals: A Review for Chemists and Non-Chemists. Part 1: Early Structural Modifications to the Nucleoside Scaffold. *Antiviral Res.* **2018**, *154*, 66−86.

(12) Peersen, O. B. A Comprehensive Superposition of Viral Polymerase Structures. *Viruses* **2019**, *11*, 745.

(13) Sheahan, T. P.; Sims, A. C.; Zhou, S.; Graham, R. L.; Pruijssers, A. J.; Agostini, M. L.; Leist, S. R.; Schäfer, A.; Dinnon, K. H.; Stevens, L. J.; Chappell, J. D.; Lu, X.; Hughes, T. M.; George, A. S.; Hill, C. S.; Montgomery, S. A.; Brown, A. J.; Bluemling, G. R.; Natchus, M. G.; Saindane, M.; Kolykhalov, A. A.; Painter, G.; Harcourt, J.; Tamin, A.; Thornburg, N. J.; Swanstrom, R.; Denison, M. R.; Baric, R. S. An Orally Bioavailable Broad-Spectrum Antiviral Inhibits SARS-CoV-2 in

Human Airway Epithelial Cell Cultures and Multiple Coronaviruses in Mice. *Sci. Transl. Med.* 2020, 12, eabb5883.

(14) Brown, A. J.; Won, J. J.; Graham, R. L.; Dinnon, K. H., III; Sims, A. C.; Feng, J. Y.; Cihlar, T.; Denison, M. R.; Baric, R. S.; Sheahan, T. P. Broad Spectrum Antiviral Remdesivir Inhibits Human Endemic and Zoonotic Deltacoronaviruses with a Highly Divergent RNA Dependent RNA Polymerase. *Antiviral Res.* 2019, 169, 104541.

(15) PDB code 6M71: Gao, Y.; Yan, L.; Huang, Y.; Liu, F.; Zhao, Y.; Cao, L.; Wang, T.; Sun, Q.; Ming, Z.; Zhang, L.; Ge, J.; Zheng, L.; Zhang, Y.; Wang, H.; Zhu, Y.; Zhu, C.; Hu, T.; Hua, T.; Zhang, B.; Yang, X.; Li, J.; Yang, H.; Liu, Z.; Xu, W.; Guddat, L. W.; Wang, Q.; Lou, Z.; Rao, Z. Structure of the RNA-Dependent RNA Polymerase from COVID-19 Virus. *Science* 2020, 368, 779.

(16) PDB code 6YYT: Hillen, H. S.; Kokic, G.; Farnung, L.; Dienemann, C.; Tegunov, D.; Cramer, P. Structure of Replicating SARS-CoV-2 Polymerase. *Nature* 2020, 584, 154–156.

(17) PDB code 7BV2: Yin, W.; Mao, C.; Luan, X.; Shen, D.-D.; Shen, Q.; Su, H.; Wang, X.; Zhou, F.; Zhao, W.; Gao, M.; Chang, S.; Xie, Y.-C.; Tian, G.; Jiang, H.-W.; Tao, S.-C.; Shen, J.; Jiang, Y.; Jiang, H.; Xu, Y.; Zhang, S.; Zhang, Y.; Xu, H. E. Structural Basis for Inhibition of the RNA-Dependent RNA Polymerase from SARS-CoV-2 by Remdesivir. *Science* 2020, 368, 1499–1504.

(18) PDB code 6NUR: Kirchdoerfer, R. N.; Ward, A. B. Structure of the SARS-CoV Nsp12 Polymerase Bound to Nsp7 and Nsp8 Co-Factors. *Nat. Commun.* 2019, 10, 2342–2349.

(19) PDB code 3BSO: Zamyatkin, D. F.; Parra, F.; Alonso, J. M. M.; Harki, D. A.; Peterson, B. R.; Grochulski, P.; Ng, K. K. S. Structural Insights into Mechanisms of Catalysis and Inhibition in Norwalk Virus Polymerase. *J. Biol. Chem.* 2008, 283, 7705–7712.

(20) Zamyatkin, D. F.; Parra, F.; Machín, Á.; Grochulski, P.; Ng, K. K. S. Binding of 2′-Amino-2′-Deoxycytidine-5′-Triphosphate to Norovirus Polymerase Induces Rearrangement of the Active Site. *J. Mol. Biol.* 2009, 390, 10–16.

(21) PDB code 4WTD: Appleby, T. C.; Perry, J. K.; Murakami, E.; Barauskas, O.; Feng, J.; Cho, A.; Fox, D.; Wetmore, D. R.; McGrath, M. E.; Ray, A. S.; Sofia, M. J.; Swaminathan, S.; Edwards, T. E. Structural Basis for RNA Replication by the Hepatitis C Virus Polymerase. *Science* 2015, 347, 771–775.

(22) Ahmad, M.; Dwivedy, A.; Mariadasse, R.; Tiwari, S.; Kar, D.; Jeyakanthan, J.; Biswal, B. K. Prediction of Small Molecule Inhibitors Targeting the Severe Acute Respiratory Syndrome Coronavirus-2 RNA-Dependent RNA Polymerase. *ACS Omega* 2020, 5, 18356–18366.

(23) Gordon, C. J.; Tchesnokov, E. P.; Woolner, E.; Perry, J. K.; Feng, J. Y.; Porter, D. P.; Götte, M. Remdesivir Is a Direct-Acting Antiviral That Inhibits RNA-Dependent RNA Polymerase from Severe Acute Respiratory Syndrome Coronavirus 2 with High Potency. *J. Biol. Chem.* 2020, 295, 6785–6797.

(24) Kokic, G.; Hillen, H. S.; Tegunov, D.; Dienemann, C.; Seitz, F.; Schmitzova, J.; Farnung, L.; Siewert, A.; Höbartner, C.; Cramer, P. Mechanism of SARS-CoV-2 Polymerase Stalling by Remdesivir. *Nat. Commun.* 2021, 12, 279.

(25) Agostini, M. L.; Pruijssers, A. J.; Chappell, J. D.; Gribble, J.; Lu, X.; Andres, E. L.; Bluemling, G. R.; Lockwood, M. A.; Sheahan, T. P.; Sims, A. C.; Natchus, M. G.; Saindane, M.; Kolykhalov, A. A.; Painter, G. R.; Baric, R. S.; Denison, M. R. Small-Molecule Antiviral β-d-N4-Hydroxycytidine Inhibits a Proofreading-Intact Coronavirus with a High Genetic Barrier to Resistance. *J. Virol.* 2019, 93, No. e01348-19.

(26) Shannon, A.; Selisko, B.; Le, N. T. T.; Huchting, J.; Touret, F.; Piorkowski, G.; Fattorini, V.; Ferron, F.; Decroly, E.; Meier, C.; Coutard, B.; Peersen, O.; Canard, B. Rapid Incorporation of Favipiravir by the Fast and Permissive Viral RNA Polymerase Complex Results in SARS-CoV-2 Lethal Mutagenesis. *Nat. Commun.* 2020, 11, 4682.

(27) Siegel, D.; Hui, H. C.; Doerffler, E.; Clarke, M. O.; Chun, K.; Zhang, L.; Neville, S.; Carra, E.; Lew, W.; Ross, B.; Wang, Q.; Wolfe, L.; Jordan, R.; Soloveva, V.; Knox, J.; Perry, J.; Perron, M.; Stray, K. M.; Barauskas, O.; Feng, J. Y.; Xu, Y.; Lee, G.; Rheingold, A. L.; Ray, A. S.; Bannister, R.; Strickley, R.; Swaminathan, S.; Lee, W. A.; Bavari, S.; Cihlar, T.; Lo, M. K.; Warren, T. K.; Mackman, R. L. Discovery and Synthesis of a Phosphoramidate Prodrug of a Pyrrolo[2,1-f][Triazin-4-Amino] Adenine C-Nucleoside (GS-5734) for the Treatment of Ebola and Emerging Viruses. *J. Med. Chem.* 2017, 60, 1648–1661.

(28) Schrödinger, LLC. *Schrödinger Release 2019-4*: Maestro. New York, NY 2019.

(29) Yang, A. S.; Honig, B. An Integrated Approach to the Analysis and Modeling of Protein Sequences and Structures. I. Protein Structural Alignment and a Quantitative Measure for Protein Structural Distance. *J. Mol. Biol.* 2000, 301, 665–678.

(30) Bruenn, J. A. A Structural and Primary Sequence Comparison of the Viral RNA-Dependent RNA Polymerases. *Nucleic Acids Res.* 2003, 31, 1821–1829.

(31) Madhavi Sastry, G.; Adzhigirey, M.; Day, T.; Annabhimoju, R.; Sherman, W. Protein and Ligand Preparation: Parameters, Protocols, and Influence on Virtual Screening Enrichments. *J. Comput.-Aided Mol. Des.* 2013, 27, 221–234.

(32) Jacobson, M. P.; Pincus, D. L.; Rapp, C. S.; Day, T. J. F.; Honig, B.; Shaw, D. E.; Friesner, R. A. A Hierarchical Approach to All-Atom Protein Loop Prediction. *Proteins* 2004, 55, 351–367.

(33) Jacobson, M. P.; Friesner, R. A.; Xiang, Z.; Honig, B. On the Role of the Crystal Environment in Determining Protein Side-Chain Conformations. *J. Mol. Biol.* 2002, 320, 597–608.

(34) Bochevarov, A. D.; Harder, E.; Hughes, T. F.; Greenwood, J. R.; Braden, D. A.; Philipp, D. M.; Rinaldo, D.; Halls, M. D.; Zhang, J.; Friesner, R. A. Jaguar: A High-Performance Quantum Chemistry Software Program with Strengths in Life and Materials Sciences. *Int. J. Quantum Chem.* 2013, 113, 2110–2142.

(35) US-FDA. *FDA Approves First Treatment for COVID-19*. https://www.fda.gov/news-events/press-announcements/fda-approves-first-treatment-covid-19.

(36) Sheahan, T. P.; Sims, A. C.; Graham, R. L.; Menachery, V. D.; Gralinski, L. E.; Case, J. B.; Leist, S. R.; Pyrc, K.; Feng, J. Y.; Trantcheva, I.; Bannister, R.; Park, Y.; Babusis, D.; Clarke, M. O.; Mackman, R. L.; Spahn, J. E.; Palmiotti, C. A.; Siegel, D.; Ray, A. S.; Cihlar, T.; Jordan, R.; Denison, M. R.; Baric, R. S. Broad-Spectrum Antiviral GS-5734 Inhibits Both Epidemic and Zoonotic Coronaviruses. *Sci. Transl. Med.* 2017, 9, eaal3653.

(37) Wang, M.; Cao, R.; Zhang, L.; Yang, X.; Liu, J.; Xu, M.; Shi, Z.; Hu, Z.; Zhong, W.; Xiao, G. Remdesivir and Chloroquine Effectively Inhibit the Recently Emerged Novel Coronavirus (2019-NCoV) in Vitro. *Cell Res.* 2020, 30, 269–271.

(38) Halford, B. *An emerging antiviral takes aim at COVID-19* https://cen.acs.org/pharmaceuticals/drug-development/emerging-antiviral-takes-aim-COVID-19/98/web/2020/05 (accessed May 25, 2020).

(39) Furuta, Y.; Komeno, T.; Nakamuba, T. Favipiravir (T-705), a Broad Spectrum Inhibitor of Viral RNA Polyermase. *Proc Jpn Acad Ser B Phys Biol Sci.* 2017, 93, 449–463.

(40) Warren, T. K.; Wells, J.; Panchal, R. G.; Stuthman, K. S.; Garza, N. L.; Van Tongeren, S. A.; Dong, L.; Retterer, C. J.; Eaton, B. P.; Pegoraro, G.; Honnold, S.; Bantia, S.; Kotian, P.; Chen, X.; Taubenheim, B. R.; Welch, L. S.; Minning, D. M.; Babu, Y. S.; Sheridan, W. P.; Bavari, S. Protection against Filovirus Diseases by a Novel Broad-Spectrum Nucleoside Analogue BCX4430. *Nature* 2014, 508, 402–405.

(41) Pruijssers, A. J.; Denison, M. R. Nucleoside Analogues for the Treatment of Coronavirus Infections. *Curr. Opin. Virol.* 2019, 35, 57–62.

(42) Peters, H. L.; Jochmans, D.; De Wilde, A. H.; Posthuma, C. C.; Snijder, E. J.; Neyts, J.; Seley-Radtke, K. L. Design, Synthesis and Evaluation of a Series of Acyclic Fleximer Nucleoside Analogues with Anti-Coronavirus Activity. *Bioorganic Med. Chem. Lett.* 2015, 25, 2923–2926.

(43) Ferron, F.; Subissi, L.; De Morais, A. T. S.; Le, N. T. T.; Sevajol, M.; Gluais, L.; Decroly, E.; Vonrhein, C.; Bricogne, G.; Canard, B.; Imbert, I. Structural and Molecular Basis of Mismatch

Correction and Ribavirin Excision from Coronavirus RNA. *Proc. Natl. Acad. Sci. U. S. A.* **2017**, *115*, E162−E171.

(44) Agostini, M. L.; Andres, E. L.; Sims, A. C.; Graham, R. L.; Sheahan, T. P.; Lu, X.; Smith, E. C.; Case, J. B.; Feng, J. Y.; Jordan, R.; Ray, A. S.; Cihlar, T.; Siegel, D.; Mackman, R. L.; Clarke, M. O.; Baric, R. S.; Denison, M. R. Coronavirus Susceptibility to the Antiviral Remdesivir (GS-5734) Is Mediated by the Viral Polymerase and the Proofreading Exoribonuclease. *MBio* **2018**, *9*, 1−15.